Constructing the Universe with Clusters of Galaxies, IAP 2000 meeting, Paris (France) July 2000
Florence Durret & Daniel Gerbal eds.

CORE WITHIN CORE IN GALAXY CLUSTERS

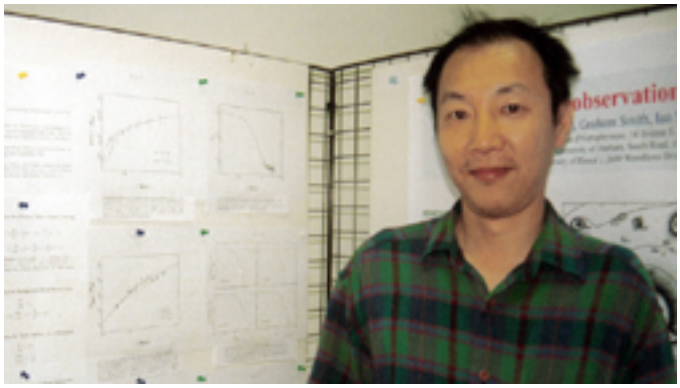

Tzihong Chiueh[1], Xiang-Ping Wu[2]
Physics Department, National Taiwan University, Taipei, Taiwan[1],
National Astronomical Observatories, Beijing 100012, China[2]

When the cold dark matter particles are allowed to relax to approach an asymptotic thermodynamic equilibrium at the cluster center via, for example, collisions or other forms of relaxation, the cluster center can develop a dense inner core, which has a size much smaller than that of the usual outer core. The cluster mass distribution for such kind of dark matter particles is constructed. Reasonable agreements are found for the predicted lensing mass, galaxy and x-ray gas distributions with the observations.

1 Introduction

The interior mass distribution within few tens of kpc from the cluster center has recently been recognized to be a puzzle. (See Wu et al. (1998)[1] and references therein.) The mass estimate from the strong lensing observations gives about twice as high a value as those derived from the weak lensing and x-ray observations. Though the discrepancy tends to diminish in the strong-cooling-flow clusters, the evidences in the non-cooling-flow clusters are convincing [2]. A possible account for this mass discrepancy can be that the cluster center contains a dense inner core, which cannot be interpolated from the mass measurements in the cluster bulk by the weak lensing and x-ray observations.

The universal distribution of the cold dark matter advocated by Narravo, Frenk and White [3] does indeed contain a density cusp, proportional to r^{-1}, at the cluster center. However, such a density singularity is too weak to contribute in any significant way to strong lensing [2]. Even for the more singular density cusp ($\propto r^{-1.5}$) recently found by high-resolution numerical simulations[4,5,6], it is still too weak for strong lensing. Unless the currently best numerical simulations for structure formation are still too inaccurate to address the gravitational dynamics within few tens of kpc from the cluster center, one needs to seek new physics in order to allow for the existence of the dense inner core. The additional piece of physics must be such that the dark matter at the cluster center is built up with efficient heat exchange with the cluster bulk. This is possible through either particle collisions[7,8]or collective waves. Since the self-gravitating system has negative heat capacity, removing the energy from the core and heating up the bulk simply make the cluster core become even more tightly bound, and drive the system closer to the asymptotic thermodynamic equilibrium. This situation is not unlike that occurs in the center of a globular cluster. However, in order to create such an environment that prompts the

gravitational system to reach this unusual state, an initial dense seed core is needed.

Below, we summarize our recent work on an infall model for the formation of a twin-core galaxy cluster seeded by an initial density peak[9]. This work incorporates the aforementioned components and intends to model a cluster with a collisional inner core and a collisionless bulk. Such a cluster presently contains a usual x-ray core of about 150 h^{-1} kpc and an inner dense core within a few kpc. Specifically, the core physics is modeled by an appropriate inner boundary condition of the bulk flow, and the cluster bulk is in turn modeled to consist of a hot isothermal gas, infalling subsonically with the heat carried from the cluster interior outwards. The isothermality arises because of the large mean-free-path and efficient heat conductivity of the dark-matter particles. Outside the cluster, the background cold dark matter falls in supersonically till it impinges onto a heat conduction front, which defines the cluster boundary. We then use the gravitational potential of the mass distribution to construct the equilibrium galaxy and gas distributions for comparisons with the observed galaxy and x-ray distributions.

2 Results and Comparisons with Observations

Figure (1) shows the scaled density $\alpha(x)$, infall velocity $v(x)$ and mass $m(x)$ distributions, where the radial distance r has been rescaled as $x \equiv r/\sigma_d\tau$, with σ_d and τ being the velocity dispersion of cluster dark matter and the time, respectively. Both outer core and inner dense core are visible in Fig.(1 a); a conduction front at $x \sim 0.7$ is also seen. The discontinuity at the conduction front should not be taken too literally and it is an artifact resulting from our treatment of dark matter as an isothermal *fluid*; in the outskirts of a cluster the dark matter should have already become collisionless and the conduction front should have been a smooth transition rather than a sharp transition. On the other hand, the sudden density rise of the inner core results from the fact that the infall speed originally approaches the sound speed near the cluster center but it gets retarded in order for the infall to land at the center at a vanishing speed. (See Fig. (1b).) In Fig.(1d), we also show the density profile of a saturated cluster where the infall has terminated. This profile is constructed by assuming that the inner core mass remains intact regardless of whether the infall has ended or not.

The galaxy distribution in the cluster can be constructed from our mass distribution by assuming that the galaxies are in virial equilibrium, where the observed galaxy velocity distribution is used as an input. Figure (2) shows the comparisons of two predicted galaxy distributions with the observed ones [10]. It shows reasonably good agreements. The x-ray surface-brightness distribution can also be predicted by assuming that the gases have a polytropic equation of state. Shown in Fig.(3) is a comparison of the predicted surface brightness with the observed one for Cl0016+16 [11]. Note that the predicted distribution can fit the β model quite well.

The predicted mass distribution can also be compared with the mass estimates derived from various strong and weak lensing measurements, and Fig.(4) shows a comparison of our result with the statistical distribution of the lensing masses of clusters [1,12]. The downward turn of the predicted mass beyond 0.5 Mpc that matches the weak lensing mass is due to the density deficiency outside the conduction front shown in Fig.(1a) for the on-going growing clusters. The saturated clusters have smooth density distributions and are not expected to have a mismatch between the strong-lensing mass and the weak lensing mass. We fix the only two free parameters, the amplitude and length scale, of our density profile from the lensing data of Fig.(4). This unique profile will be used for further comparisons with the observed statistical distributions of tracers in clusters.

Our expected result for the statistical distribution of galaxies in clusters on average is plotted in Fig.(5); it is compared with the CNOC galaxies[13]. Again, a reasonable agreement is found. For the x-ray gases in clusters, we may again assume the cluster gases are polytropic and construct the expected gas distribution to be compared with that of the β models, which have been found

to fit the x-ray surface brightness remakably well. To constrain the gas parameters, we demand that the mean kinetic energy per mass for dark matter particles is the same as that for the gas. Various polytropic indices are used, and they seem to agree well with the β models of various β's , as revealed in Fig.(6). For $\beta = 2/3$, the average β value of most clusters, we find that the polytropic index $\gamma = 1.2$.

3 Concluding Remaks

Finally, we discuss why the strong cooling-flow clusters tend not to have mass discrenpacy but the non-cooling-flow clusters do, as suggested by observations. It is known that the cooling-flow clusters are rich clusters, which have formed long ago. Therefore the cooling-flow clusters are saturated clusters, and the non-cooling-flow clusters are on-going growing clusters. The on-going growing cluster has a conduction front in the outskirts surrounded by a lower-density cold background in its immediate neighborhood, and therefore the mass determination through weak lensing measurements can be smaller by a factor of two, c.f., Fig.(4).

An alternative explanation for this problem can be that the cooling-flow cluster does not contain an inner core at all. It can be due to that the cooling flow clusters are old rich clusters, therefore having a higher chance to accrete clusters of comparable sizes in the past. The kinetic energy pertinent to the violent major mergers may eventually penertrate into the original inner dense cores, thereby evaporating them. The system then bifurcates away from the configurations accessible to the asymptotic thermodynamical equilibrium, at least within the Hubble time scale. By contrast, the non-cooling-flow clusters are young, and formed mostly through the quiescent growth, as represented by our model with infall of the surrounding small clumps. It is therefore conceivable that the dense inner cores are not too much disturbed to dissappear.

References

1. X.P. Wu, T. Chiueh, L.Z. ang and Y.J. Xue, MNRAS, 301, 861 (1998)
2. X.P. Wu, MNRAS (in press), astro-ph/0006124
3. J.F. Narravo, C.S. Frenk and S.D.M. White, MNRAS, 275, 720 (1995)
4. T. Fukushige and J. Makino, ApJ, 477, L9 (1997)
5. B. Moore, T. Quinn, F. Governato, J. Stadel and G. Lake, MNRAS, 310, 1147 (1999)
6. Y.P. Jing and Y. Suto, ApJ, 529, L69 (2000)
7. D.N. Spergel and P.J. Steinhardt, Phys. Rev. Lett., 84, 376 (2000)
8. B. Moore, S. Gelato, A. Jenkins, F.R. Pearce and V. Quilis, ApJ, 535, L21 (2000)
9. T. Chiueh and X.P. Wu, A&A, 353, 823 (2000)
10. D. Clow, G.A. Luppino, N. Kaiser, J.P. Henry and I.M. Gioia, ApJ, 497, L61
11. D.M. Neumann and H. Böhringer, MNRAS, 289, 123 (1997)
12. A.N. Taylor, S. Dye, T.J. Broadhurst, N. Benitez and E. van Kampen, ApJ, 501, 539 (1998)
13. R.G. Carlberg, H.K.C. Yee and E. Ellingson, ApJ, 478, 462 (1997)

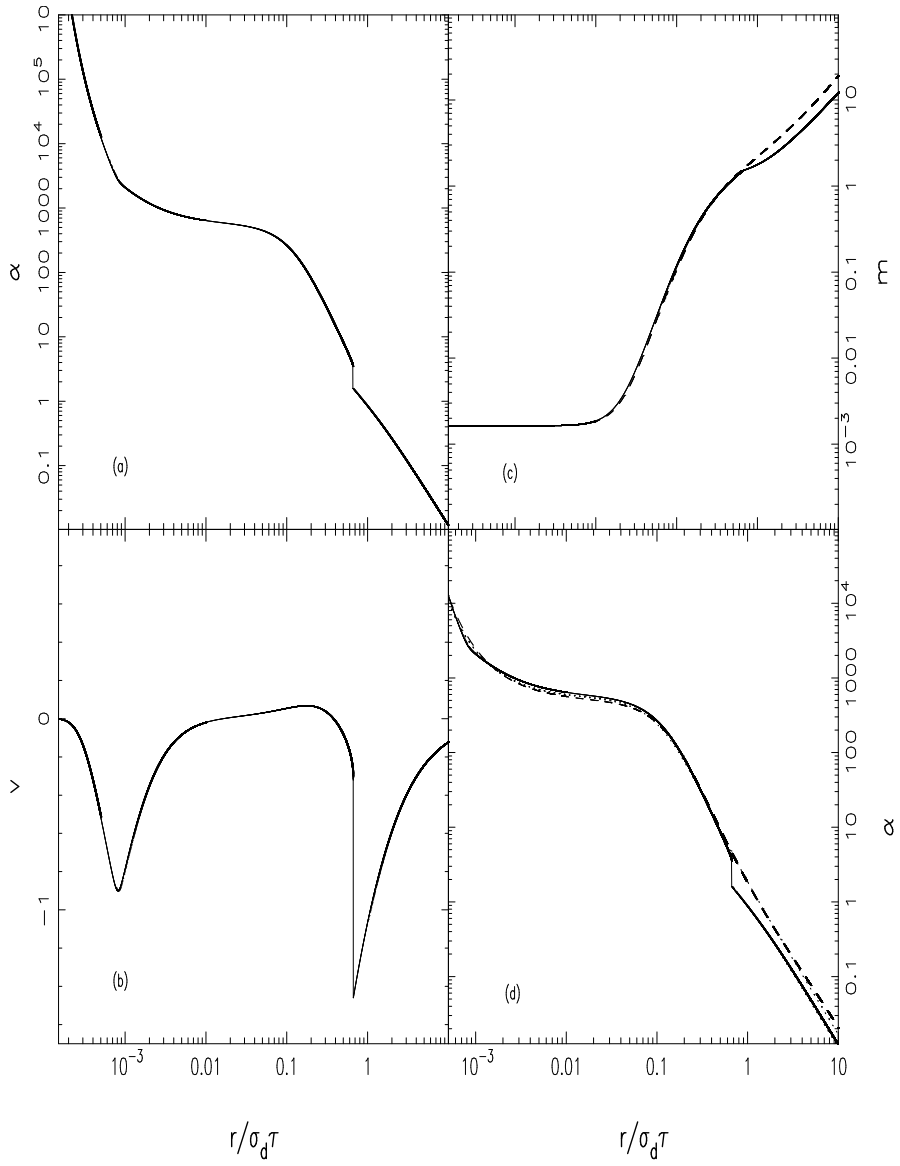

Figure 1: (a)Dimensionless density profile, (b)flow speed and (c) cluster mass obtained from the recent-infall, self-similar solutions under the initial and boundary conditions of a mass concentration $m_0 = 1.6 \times 10^{-3}$ within $x = r/\sigma_d\tau = 0.0005$. Also shown are the density (d) and mass (c) variations for a saturated cluster (dashed lines) expected under the same inner boundary condition. Analytic fits of the density profiles can be obtained and shown with dotted lines.

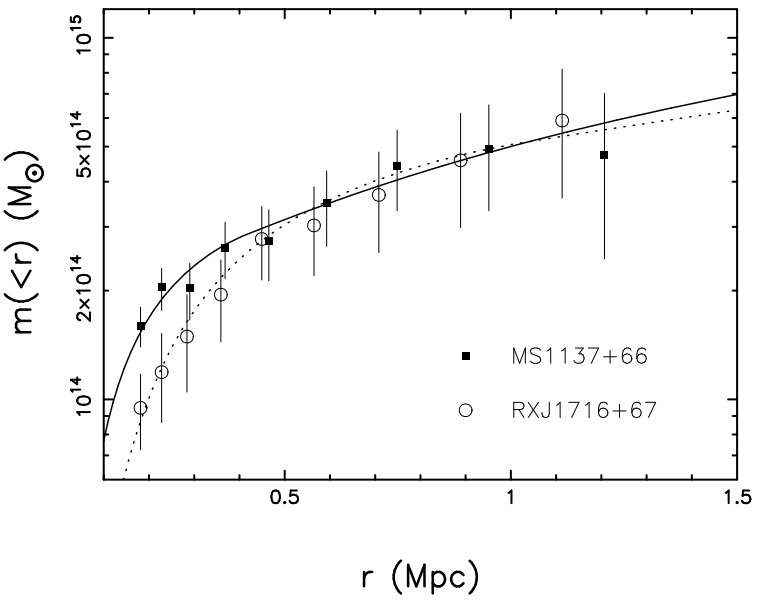

Figure 2: A comparison between the projected cluster masses derived from the weakly distorted images of background galaxies behind clusters MS1137+66 and RXJ1716+67 and those from our saturation model. Data sets of the lensing cluster masses are from Clowe et al. (1988). Our best fitting yields $(\sigma_d, \sigma_d\tau) = (850$ km s^{-1},1.5 Mpc) and $(\sigma_d, \sigma_d\tau) = (1000$ km s^{-1},0.6 Mpc) for MS1137+66 and RXJ1716+67, respectively.

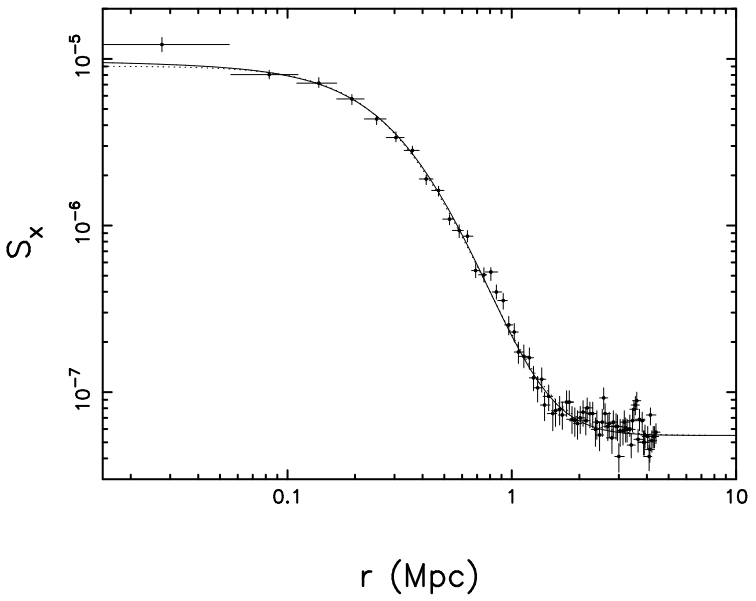

Figure 3: An examples of fit of the theoretically predicted X-ray surface brightness (solid lines) to the observation of Cl0016+16 (Neumann & Böhringer 1997). The best β model fit is also displayed (dotted lines) for comparison. A background surface brightness of 5.5×10^{-8} s^{-1} arcsec^{-2} is assumed.

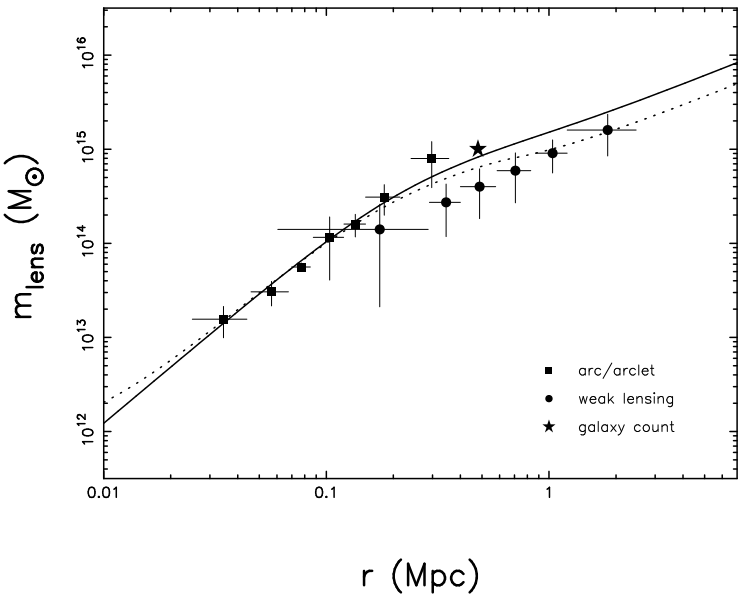

Figure 4: An overall radial variation of the projected cluster masses revealed by the gravitational lensing methods: the strongly (arcs/arclets) and weakly distorted images of background galaxies (for references see Wu et al. 1998) as well as the deficit of red galaxies behind A1689 (Taylor et al. 1998). The results predicted by the recent-infall solution (dotted line) and the saturated configuration (solid line) are shown for $\sigma_d = 1300$ km s^{-1} and $\sigma_d \tau = 1$ Mpc.

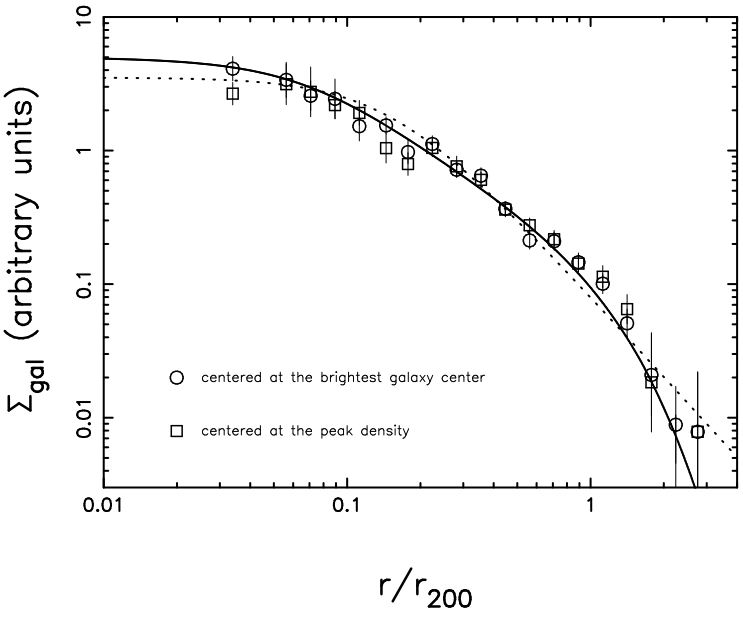

Figure 5: Surface number density profile of galaxies over an ensemble of 14 distant clusters from CNOC (Carlberg, Yee, & Ellingson 1997). Solid line is our expected result of the saturation model for $\sigma_d/\sigma_{gal}(0) = 0.78$ and $r_{200}/\sigma_d\tau = 0.4$ under the assumption that galaxies trace the gravitational potential of dark matter particles in clusters. The conventional King model fit is illustrated by the dotted line.

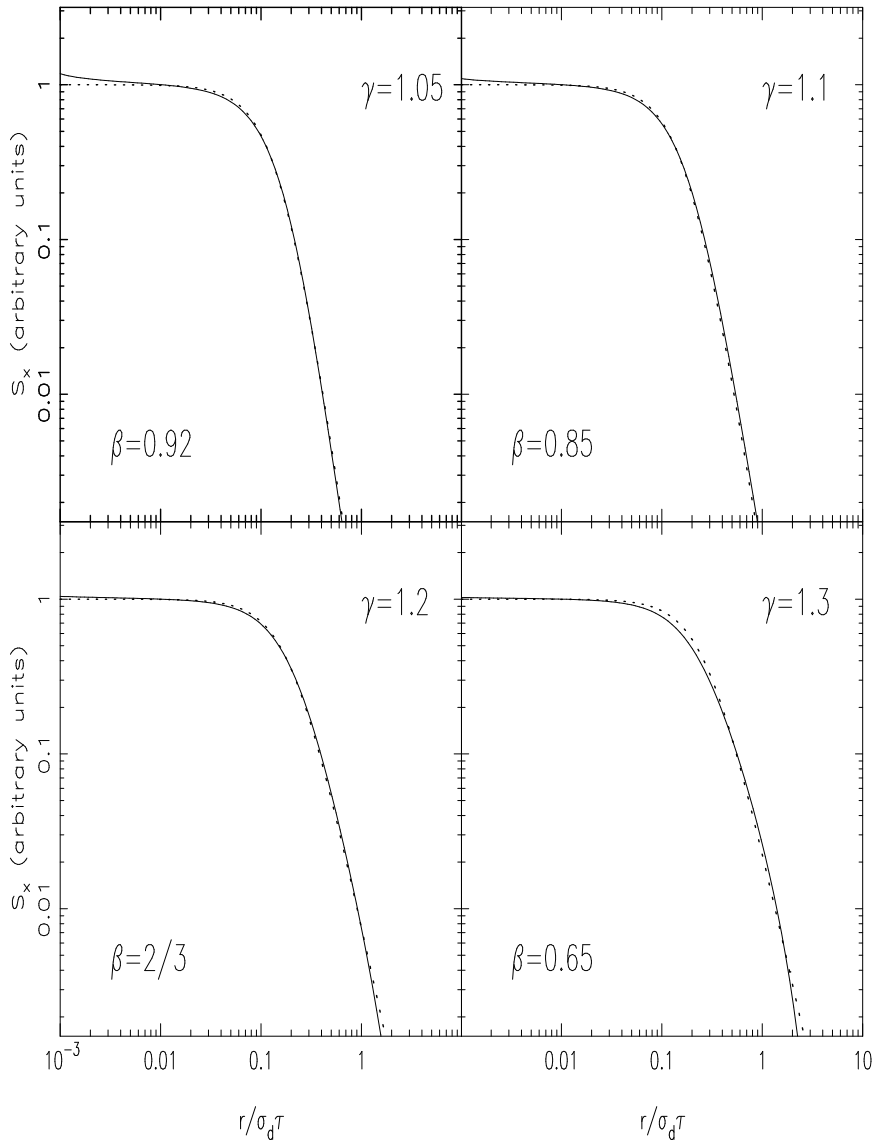

Figure 6: X-ray surface brightness profiles predicted for different polytropic indices $\gamma = 1.05$ 1.1, 1.2 and 1.3 in the equation of state $T \propto n^{\gamma-1}$ (solid lines). The requirement that the mean kinetic energy of dark matter particles is equal to that of gas, $\sigma_d^2 = (k\overline{T}/\mu m_p)$ has been employed. Also plotted are the conventional β gas profiles (dotted lines).